Available online at www.sciencedirect.com
ScienceDirect
Journal of Hazardous Materials 153 (2008) 1301–1307
Journal of Hazardous Materials
www.elsevier.com/locate/jhazmat

Calculation of the upper flammability limit of methane/air mixtures at elevated pressures and temperatures

F. Van den Schoor [a,*], F. Verplaetsen [b], J. Berghmans [a]

[a] *Katholieke Universiteit Leuven, Department of Mechanical Engineering, Celestijnenlaan 300A, B-3000 Leuven, Belgium*
[b] *Adinex N.V., Brouwerijstraat 5/3, 2200 Herentals, Belgium*

Received 30 July 2007; accepted 24 September 2007
Available online 29 September 2007

Abstract

Four different numerical methods to calculate the upper flammability limit of methane/air mixtures at initial pressures up to 10 bar and initial temperatures up to 200 °C are evaluated by comparison with experimental data. Planar freely propagating flames are calculated with the inclusion of a radiation heat loss term in the energy conservation equation to numerically obtain flammability limits. Three different reaction mechanisms are used in these calculations. At atmospheric pressure, the results of these calculations are satisfactory. At elevated pressures, however, large discrepancies are found. The spherically expanding flame calculations only show a marginal improvement compared with the planar flame calculations. On the other hand, the application of a limiting burning velocity with a pressure dependence $S_{u,lim} \sim p^{-1/2}$ is found to predict the pressure dependence of the upper flammability limit very well, whereas the application of a constant limiting flame temperature is found to slightly underestimate the temperature dependence of the upper flammability limit.

Keywords: Flammability limits; Methane

1. Introduction

In a previous study [1], four different methods for the calculation of flammability limits were evaluated based both upon a comparison of their intrinsic capabilities of capturing the different aspects of a near-limit flame relevant to its extinction (Table 1), as upon a comparison of their results with experimental data on the (lower and upper) flammability limits of methane/hydrogen/air mixtures at atmospheric pressure and ambient temperature. It was found among others that the estimates of the flammability limits become more accurate as more flame aspects are taken into account by the calculations. To further corroborate the previous findings, the focus of this study will be on the upper flammability limits of methane/air mixtures at initial pressures up to 10 bar and initial temperatures up to 200 °C. To this end, the results of the different numerical methods – namely the calculation of planar [2–5] and of spherical [6] flames with the inclusion of a (radiation) heat loss term in the energy conservation equation, and the application of a limiting burning velocity [4,7] and of a limiting flame temperature [8,9] – will be compared with experimental data [10].

2. Numerical methods

The calculations are performed using CHEM1D [11], a one-dimensional flame code capable of solving 1D mass, energy and species conservation equations with detailed transport and chemical kinetics models. Two different flame geometries are used, namely 1D planar premixed flames, both steady and unsteady, and quasi 1D spherically expanding premixed flames. The density, the temperature and the species mass fractions are specified at the cold boundary, while vanishing gradients are imposed at the hot boundary. Throughout the calculations it is assumed that the gas mixture is ideal and that the pressure is constant in space and time. These are valid approximations since the compressibility factor $Z \approx 1.00$ for the mixtures under consideration [12] and since the pressure increase during near-limit

* Corresponding author. Tel.: +32 16 32 25 49; fax: +32 16 32 29 85.
E-mail address: Filip.VandenSchoor@mech.kuleuven.be (F. Van den Schoor).

0304-3894/$ – see front matter © 2007 Elsevier B.V. All rights reserved.
doi:10.1016/j.jhazmat.2007.09.088

Table 1
Comparison of the different numerical methods based upon their intrinsic capabilities of capturing the different aspects of a near-limit flame that are relevant to its extinction

Flame aspects	Planar	Spherical	$S_{u,lim}$	$T_{f,lim}$[a]
Chemical kinetics	√	√	√	√
Heat loss	√	√	√	√
Flow strain			√	
Flame curvature		√		
Natural convection			√	
Flame front instabilities				
Preferential diffusion				

[a] Strictly speaking the application of a limiting flame temperature should not have been included into this comparison since it is empirically based and, therefore, difficult to ascertain which flame aspects are taken into account by it.

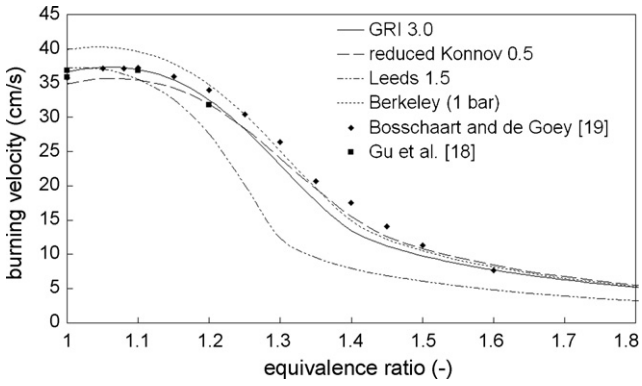

Fig. 1. Comparison between experimentally determined and calculated adiabatic burning velocities of rich methane/air flames at 1 atm and 25 °C.

flame propagation is limited to approximately 5 % of the initial pressure [10]. Further details about the flame code can be found elsewhere [13].

The radiation heat loss is modelled by means of the optically thin limit. Four radiating species are considered, namely CO_2, H_2O, CO and CH_4.

Since it is expected that the chemical kinetics play an important role in the limit flame behaviour, different reaction mechanisms will be used in the flame calculations: the GRI 3.0 mechanism [14], the Konnov 0.5 mechanism [15], a mechanism by Appel et al. [16], which will be called the Berkeley mechanism in the remainder of this paper, and the Leeds 1.5 mechanism [17].

The GRI 3.0 mechanism is widely used. Since the nitrogen chemistry is unimportant for the limits under consideration, it is removed from the base mechanism. The resulting mechanism contains 219 elementary reactions among 36 species. It can only be used for the calculation of methane and natural gas flames.

The Konnov mechanism contains 776 elementary reactions among 93 species (not including the nitrogen chemistry). It can be used for the calculation of hydrogen, carbon monoxide, methane, methanol, C_2 and C_3 hydrocarbons and their derivatives. To reduce the computational time and to allow a better comparison with the GRI mechanism, the C_3–C_6 species other than C_3H_8 and n-C_3H_7, are removed from the Konnov mechanism, leading to a reduced Konnov mechanism with 456 elementary reactions among 54 species, which will be used alongside the full mechanism.

The Berkeley mechanism contains 544 elementary reactions among 101 species. It can be used for the calculation of methane, ethane, ethylene and acetylene flames at 1 bar. There also exists a modification of this mechanism for calculating flames at 10 bar, which contains a different set of 546 elementary reactions.

The Leeds 1.5 mechanism contains 175 elementary reactions among 37 species. It can be used for the calculation of methane, ethane and ethylene flames.

The GRI mechanism is chosen because it is widely used. The Konnov, Berkeley and Leeds mechanisms are chosen in addition to the GRI mechanism to investigate not only the effect of different reaction rate parameters, but also that of a different set of species. Compared to the GRI mechanism, the Konnov mechanism includes a number of C_3–C_6 species, while the Berkeley mechanism includes aromatic species in order to better model soot formation.

These reaction mechanisms were all validated against a variety of experimental data, including burning velocities, ignition delay times and species concentration profiles [14–17]. The most important parameter of these regarding the calculation of flammability limits is the burning velocity. Therefore, the different mechanisms are tested on their ability of reproducing burning velocities of rich methane/air flames. To this end, one-dimensional planar adiabatic flames are calculated at 1 atm and 25 °C. As can be seen in Fig. 1, the calculated adiabatic burning velocities obtained with the Leeds mechanism are in poor agreement with the experimentally determined values [18,19]. Consequently, this mechanism is not used in any of the further calculations as it would considerably underestimate the upper flammability limit.

The flammability limits for the planar flames are determined by considering whether a transient flame calculation reaches a steady state or not. In the latter case, the maximum flame temperature and the burning velocity will decrease continuously in time [2]. In the spherical flame calculations, the gas mixture is ignited by means of a source term in the energy conservation equation. This ignition source is modelled as an energy input of 10.5 J during a period of 40 ms in a spherical volume with a diameter of 10 mm. These parameters are chosen to resemble the ignition source that is used in the experiments [10] with which the calculations will be compared. Mixtures in which flames propagate a distance of 100 mm are considered to be flammable.

The planar flame calculations (with the inclusion of the radiation heat loss term in the energy conservation equation) will also be used to determine values for the burning velocity and the maximum flame temperature which enable evaluation of the limiting burning velocity and limiting flame temperature approaches.

It is difficult to ascertain the uncertainty in the calculations caused by uncertainties in the reaction rate parameters, in the transport properties, etc. The comparison and the evaluation of the different numerical methods is, however, not biased by any modelling uncertainty.

Further details about the numerical methods can be found elsewhere [1].

3. Theoretical background

In the previous study [1], it was found that a constant limiting burning velocity of 5 cm/s predicts the upper flammability limit of methane/hydrogen/air mixtures at atmospheric pressure and ambient temperature very well. At elevated pressures, however, Huang et al. [4] found that the application of a constant limiting burning velocity significantly underestimates the flammability limits of highly diluted *n*-butane/air mixtures. They argued that this discrepancy is caused by the fact that the mass burning rate, rather than the burning velocity, is the eigenvalue of the flame equations. They, thus, concluded that a constant limiting burning velocity should not be used as a means to calculate the pressure dependence of the flammability limits. Although they arrived at the right conclusion, they did not acknowledge the derivation of Buckmaster and Mikolaitis [20] for the limiting burning velocity, which clearly shows its pressure dependence.

For a two-reactant mixture and a single-step reaction and for a flame propagating in an axisymmetric stagnation point flow, Buckmaster and Mikolaitis calculated the limiting (minimum) value of the Karlovitz number $\mathrm{Ka}_{\mathrm{lim}}$ that leads to extinction:

$$\mathrm{Ka}_{\mathrm{lim}} = \frac{\pi}{4}\exp\left[-\frac{1}{2}\left(1-\frac{1}{Le}\right)\frac{E_a}{RT_f^2}(T_f-T_u)\right] \quad (1)$$

with Le the Lewis number, E_a the overall activation energy, R the universal gas constant, T_f the flame temperature and T_u the temperature of the unburned gases. Based upon Eq. (1), an expression for the limiting burning velocity $S_{u,\mathrm{lim}}$ can be derived [20,21]:

$$S_{u,\mathrm{lim}} \sim \exp\left[\frac{1}{4}\left(1-\frac{1}{Le}\right)\frac{E_a}{RT_f^2}(T_f-T_u)\right]\alpha^{1/2}K^{1/2} \quad (2)$$

with α the thermal diffusivity and K the flame stretch rate. By assuming in Eq. (2) that the Zeldovich number $Ze = E_a/[RT_f^2(T_f-T_u)]$ is (nearly) pressure independent or that Le is (close to) 1, and that K is (nearly) pressure independent, the pressure dependence of the limiting burning velocity $S_{u,\mathrm{lim}}$ is given by

$$S_{u,\mathrm{lim}} \sim \alpha^{1/2} \sim p^{-1/2} \quad (3)$$

with p the pressure.

The assumption of a pressure independent flame stretch rate K is based upon the following considerations. For near-limit flames, which only propagate upwards, the flame stretch rate is proportional to the upward velocity of the flame kernel. Crescitelli et al. [22] found that the upward velocity v of a spherical flame kernel with neglect of the drag force is given by

$$v = \frac{((\rho_u/\rho_b)-1)gt}{4(1+(1/2)(\rho_u/\rho_b))} \quad (4)$$

with ρ_u and ρ_b the densities of the unburned and burned gases respectively, g the gravitational acceleration and t time. For an isobaric change of state, it is found that

$$\frac{\rho_u}{\rho_b} \sim \frac{T_f}{T_u}. \quad (5)$$

Since the (adiabatic) flame temperature T_f increases only slightly with increasing pressure [23], this density ratio is nearly pressure independent. Consequently, the upward velocity v and hence the flame stretch rate K are likewise nearly pressure independent.

Since – in addition to the pressure independent flame stretch rate – the Lewis number for the near-limit methane/air mixtures under investigation is found to be close to one: $Le = 1.1$, Eq. (3) can be used in this study to calculate the limiting burning velocity at elevated pressures based upon its value at atmospheric pressure.

4. Results

4.1. Planar and spherical flame calculations

At an initial pressure of 1 atm, the one-dimensional planar flame calculations show satisfactory agreement with the experiments (Fig. 2). All of the tested reaction mechanisms predict the slope of the temperature dependence of the upper flammability limit well, whereas the observed differences between the calculated and the experimentally determined values are approximately 2 mol.%. At an initial pressure of 10 bar, however, larger differences are found between the numerical and experimental results as well as large discrepancies between the different reaction mechanisms (Fig. 3). Moreover, all of the reaction mechanisms overestimate the slope of the temperature dependence. At an initial temperature of 25 °C, it can be seen that the Konnov mechanism reproduces the slope of the pressure dependence fairly well, whereas the results of the GRI mechanism substantially diverge from the experimental ones (Fig. 4). These large differences between the calculated and the experimentally determined values at higher pressures and temperatures imply that the estimates of the upper flammability limits obtained by one-dimensional planar flame calculations are of limited value at these conditions.

Because of computational difficulties, only a limited number of spherical flame calculations have been performed using the GRI mechanism (Table 2). They show only a slight lowering

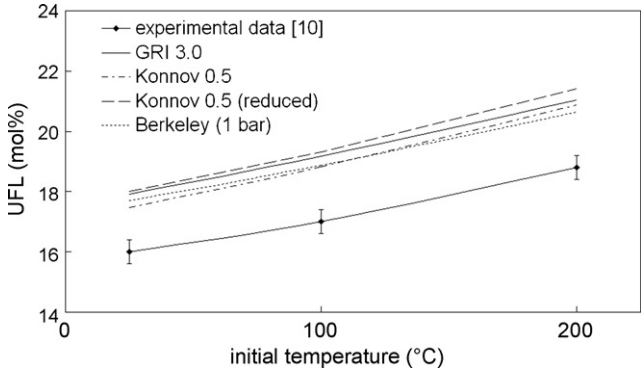

Fig. 2. Comparison between experimentally determined and calculated upper flammability limits of methane/air mixtures at 1 atm.

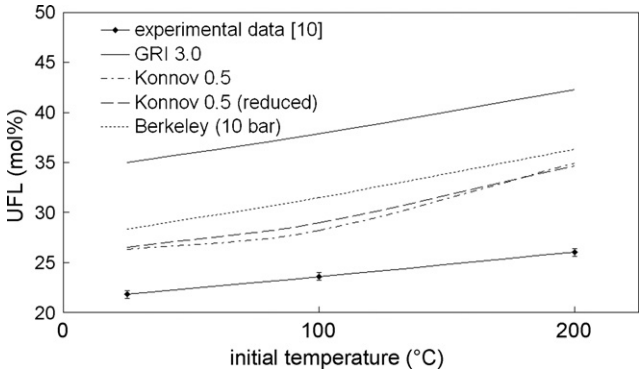

Fig. 3. Comparison between experimentally determined and calculated upper flammability limits of methane/air mixtures at 10 bar.

(of about 1 mol.%) of the calculated upper flammability limits, when referred to those of the planar flame calculations. At higher pressures and temperatures, however, this small improvement does not outweigh the increased computational effort.

The observed discrepancies between the results obtained with the different reaction mechanisms merit further analysis. Therefore, a sensitivity analysis and a reaction path analysis are performed for a methane/air flame with a methane concentration of 25.7 mol.% at an initial pressure of 10 bar and an initial temperature of 25 °C.

Sensitivity analysis can be used to identify the reactions that influence the flame behaviour the most when the flame temperature is lowered. This is done by calculating the sensitivity of the mass burning rate $\dot{m}$ on the pre-exponential reaction rate parameter A for all reactions

$$\frac{\partial \ln(\dot{m})}{\partial \ln(A)}.$$

The influence of the flame temperature on the reaction rate is, thus, simulated by a change in A.

In a reaction path analysis, the contributions of all reactions to the consumption (or formation) of a chemical species are determined by the production rates. This allows the identification of the key reactions in the transformation of the reactants into the products and the subsequent construction of a reaction path diagram.

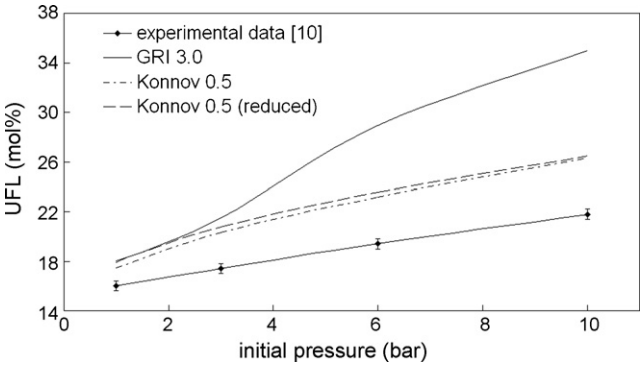

Fig. 4. Comparison between experimentally determined and calculated upper flammability limits of methane/air mixtures at 25 °C.

Table 2
Comparison of upper flammability limit values (mol.%) of methane/air mixtures obtained from planar and spherical flame calculations with experimental data

	Planar flame	Spherical flame	Experimental [10]
1 atm 25 °C	17.9	16.6 ± 0.4[a]	16.0 ± 0.4
3 bar 25 °C	21.5	20.8 ± 0.3	17.4 ± 0.4
6 bar 25 °C	28.9	28.0 ± 0.3	19.4 ± 0.4
1 atm 100 °C	19.2	18.1 ± 0.4	17.0 ± 0.4
3 bar 100 °C	23.4	22.7 ± 0.3	19.0 ± 0.4
1 atm 200 °C	21.0	20.1 ± 0.3	18.8 ± 0.4

[a] The uncertainties on the results of the spherical flame calculations stem from the concentration step size used in the calculations.

Fig. 5 shows the reactions that exhibit the largest positive and negative sensitivities, meaning that variations in their reaction rates have the largest impact on the mass burning rate. The important chain branching reaction

$$H + O_2 \rightleftharpoons O + OH$$

is found to have a large positive sensitivity for all three reaction mechanisms. Nevertheless, it is not the most important reaction in the Berkeley and GRI mechanisms as the reaction

$$CH_3 + HO_2 \rightleftharpoons CH_3O + OH$$

has a larger positive sensitivity. The complete sensitivity analysis shows an increased importance of reactions involving the HO_2 radical at elevated initial pressures. Egolfopoulos et al. [5] reached the same conclusion for lean methane/air flames. Furthermore, it can be seen that the reaction

$$CH_3 + O_2 \rightleftharpoons CH_2O + OH$$

plays an important role in the Konnov mechanism, whereas its role in the Berkeley and GRI mechanisms is rather limited. This finding is corroborated by the results of the reaction path analysis, which show that in the Konnov mechanism $CH_3 \rightarrow CH_3O \rightarrow CH_2O$ and $CH_3 \rightarrow CH_2O$ are equally important pathways, whereas in the GRI mechanism only the first is important (Fig. 6).

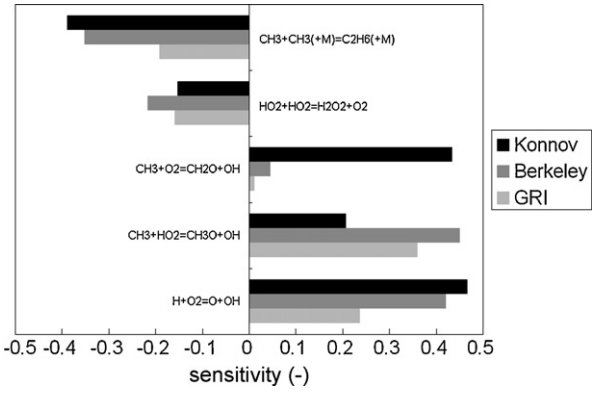

Fig. 5. Sensitivity of the mass burning rate on the reaction rate parameters of different reaction mechanisms for a methane/air flame with a methane concentration of 25.7 mol.% at 10 bar and 25 °C.

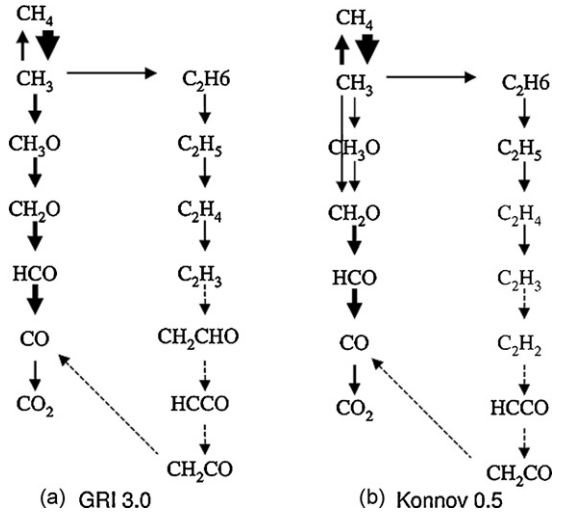

Fig. 6. Comparison of the main reaction pathways of the GRI (a) and Konnov (b) mechanism in the oxidation of CH_4 to CO and CO_2 for a methane/air flame with a methane concentration of 25.7 mol.% at 10 bar and 25 °C.

The reactions that exhibit the largest negative sensitivity are the same for all three-reaction mechanisms, namely

$$CH_3 + CH_3(+M) \rightleftharpoons C_2H_6(+M)$$

and

$$HO_2 + HO_2 \rightleftharpoons H_2O_2 + O_2.$$

There is, however, a large difference between the GRI mechanism and the Konnov mechanism regarding the sensitivity of the first reaction.

The reaction path analysis shows that despite the large difference in the number of species between the GRI (36) and the Konnov (93) mechanism, the main pathways for the oxidation of CH_4 to CO and CO_2 are very similar (Fig. 6). The presence of C_3–C_6 species in the Konnov mechanism is, thus, of minor importance for the calculation of rich methane/air flames. Therefore, it is not surprising that the results of the reduced Konnov mechanism – from which these species were removed – are nearly equal to those of the full mechanism (Figs. 2–4). This also means that the large differences between the upper flammability limits calculated with the GRI and the Konnov mechanism that are observed at elevated pressures (Fig. 4) are probably caused by a difference in reaction rate parameters, rather than by a difference in the set of elementary reactions.

The observation that the results obtained with the Konnov mechanism agree better with the experimental data does not necessarily mean that this reaction mechanism is to be preferred over the GRI mechanism, given the large differences between the numerical and experimental flames. Unfortunately, no experimental data are available on planar or spherical methane/air flames near the upper flammability limit at elevated pressures. However, there is an important difference in how these mechanisms were constructed that determines their applicability at elevated pressures. Whereas the reaction rate parameters of the GRI mechanism were fitted to the experimental data, those of the Konnov mechanism were determined a priori and only afterwards was the mechanism validated by means of the experimental data. This implies that the GRI mechanism can only be used confidently within the pressure and temperature range of the experimental data used for its construction. The Konnov mechanism, however, can be used with more confidence outside its validation range. This is the primary reason why the Konnov mechanism will be used in the subsequent calculations.

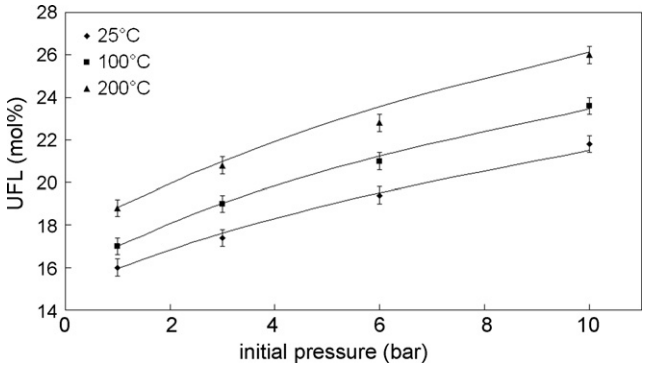

Fig. 7. Comparison of the experimentally determined upper flammability limit (markers) [10] and the pressure dependence estimated based upon the limiting burning velocity approach (solid lines) for methane/air flames.

4.2. Limiting burning velocity

At atmospheric pressure and ambient temperature, a value of 4.8 cm/s is found for the burning velocity at the experimentally determined upper flammability limit using the reduced Konnov mechanism. The theoretical derivation in Section 3 gives the pressure dependence of the limiting burning velocity (Eq. (3)). Using this equation, an estimate of the upper flammability limit at elevated pressures can be obtained starting from the experimentally determined value at atmospheric pressure. First, the burning velocity at the experimentally determined flammability limit at atmospheric pressure is calculated. Next, Eq. (3) is used to calculate the limiting burning velocity at the desired initial pressure and finally, the corresponding fuel concentration is calculated. Fig. 7 shows a comparison between the experimental data, indicated by the markers, and the results of this calculation, indicated by the full lines. Given the inaccuracies in the experimental determination of the flammability limits and in the calculation of burning velocities, as well as the assumptions made in the derivation of the limiting burning velocity, the agreement is very good.

Whereas the pressure dependence of the limiting burning velocity can easily be deduced, its temperature dependence is more complicated. For example, the flame stretch rate K experienced by a flame kernel propagating upwards cannot be assumed to be temperature independent. Therefore, another approach is used to ascertain whether the exponent a of the power dependence $S_{u,lim} \sim T^a$ is nearly constant for different pressures by calculating the burning velocity at the experimentally determined upper flammability limits and by subsequently fitting the power dependence to these data points by means of the least squares method. a is found to lie in the range 0.96–1.18 for pressures up to 10 bar. Compared to the pressure dependence for which a similar exercise with $S_{u,lim} \sim p^b$

Table 3
Calculated flame temperature (K) at the experimentally determined upper flammability limits of methane/air mixtures at different initial pressures and temperatures

	298 K	373 K	473 K
1 atm	1692	1678	1667
3 bar	1648	1622	1612
6 bar	1597	1583	1584
10 bar	1545	1533	1524

gives $b = -0.50 \pm 0.02$, the spread on a is too large to be useful. This comparison, however, only shows that the temperature dependence of the limiting burning velocity does not follow a simple power dependence, as opposed to its pressure dependence. Consequently, more research is necessary to explore the applicability of the limiting burning velocity approach to predict the temperature dependence of the flammability limits. In the next section, it will be shown that the limiting flame temperature concept offers a better potential to estimate the temperature dependence.

4.3. Limiting flame temperature

Calculation of the maximum flame temperatures at the experimentally determined upper flammability limits shows that the limit flame temperature remains nearly constant for a given initial pressure, independent of initial temperature (Table 3). Using the concept of a constant limiting flame temperature, an estimate of the upper flammability limit at elevated temperatures can be obtained starting from the experimentally determined value at ambient temperature. Fig. 8 shows a comparison between the experimental data, indicated by the markers, and the results of this calculation, indicated by the full lines. It can be seen that the use of a constant limiting flame temperature to estimate the temperature dependence of the upper flammability limit leads to slight underestimations at elevated temperatures. Moreover, it must be emphasised that using this approach to estimate the pressure dependence would lead to large underestimations at elevated pressures as the calculated flame temperatures at the experimentally determined upper flammability limits decrease by approximately 150 °C in the pressure range 1–10 bar (Table 3).

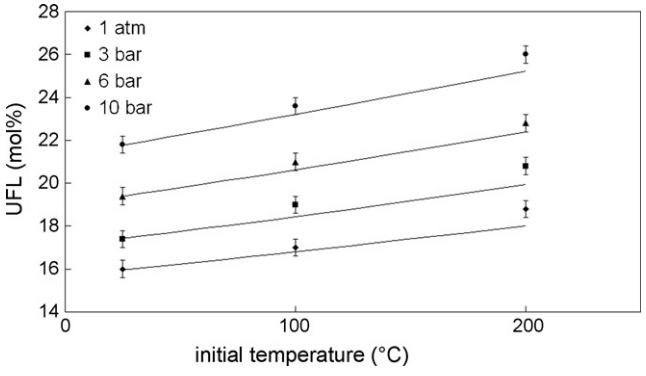

Fig. 8. Comparison of the experimentally determined upper flammability limit (markers) [10] and the temperature dependence estimated based upon the limiting flame temperature approach (solid lines) for methane/air flames.

5. Discussion

The findings of this study corroborate those of the previous study [1]. Specifically, they show that the concept of a limiting burning velocity (derived from a limiting Karlovitz number) has the best potential for accurately calculating the flammability limits. This is not surprising since – as was described in detail in the previous study – this approach takes most of the aspects of a near-limit flame that are relevant to its extinction into account, as can be seen in Table 1. It must, however, be borne in mind – as can be deduced from Table 1 – that none of the methods will give satisfactory results if flame front instabilities are present. Nevertheless, this study has shown that the concept of a limiting burning velocity cannot only be used to estimate the flammability limits at atmospheric pressure and ambient temperature, but also at elevated pressures (and temperatures).

6. Conclusions

It is found that for rich methane/air mixtures:

(1) At atmospheric pressure, the calculation of the upper flammability limit by calculating planar flames with the inclusion of radiation heat loss is satisfactory. The differences between the reaction mechanisms are minimal.
(2) At elevated pressures, the calculated upper flammability limit values are significantly too high and large differences are found between the different reaction mechanisms. The results obtained with the (reduced) Konnov mechanism show the best agreement with the experimental data.
(3) The spherical flame calculations show a marginal improvement compared with the planar flame calculations.
(4) The application of a limiting burning velocity with a pressure dependence $S_{u,lim} \sim p^{-1/2}$ gives good agreement with the experimental data.
(5) The application of a constant limiting flame temperature slightly underestimates the temperature dependence of the upper flammability limit, while it considerably underestimates its pressure dependence.

Acknowledgements

A preliminary version of this paper was presented at the 12th International Symposium on Loss Prevention and Safety Promotion in the Process Industries [24].

References

[1] F. Van den Schoor, R.T.E. Hermanns, J.A. van Oijen, F. Verplaetsen, L.P.H. de Goey, Comparison and evaluation of methods for the determination of flammability limits, applied to methane/hydrogen/air mixtures, J. Hazard. Mater. 150 (2008) 573–581.
[2] K.N. Laksmisha, P.J. Paul, H.S. Mukunda, On the flammability limit and heat loss in flames with detailed chemistry, in: Proceedings of the 23rd Symposium on Combustion, The Combustion Institute, 1990, pp. 433–440.

[3] J. Yiguang, G. Masuya, P.D. Ronney, Effects of radiative emission and absorption on the propagation and extinction of premixed gas flames, in: Proceedings of the 27th Symposium on Combustion, The Combustion Institute, 1998, pp. 2619–2626.
[4] Y. Huang, C.J. Sung, J.A. Eng, Dilution limits of *n*-butane/air mixtures under conditions relevant to HCCI combustion, Combust. Flame 136 (2004) 457–466.
[5] F.N. Egolfopoulos, A.T. Holley, C.K. Law, An assessment of the lean flammability limits of CH_4/air and C_3H_8/air mixtures at engine-like conditions, in: Proceedings of the 31st Symposium on Combustion, The Combustion Institute, 2007, pp. 3015–3022.
[6] M. Sibulkin, A. Frendi, Prediction of flammability limit of an unconfined premixed gas in the absence of gravity, Combust. Flame 82 (1990) 334–345.
[7] M.N. Bui-Pham, J.S. Miller, Rich methane/air flames: burning velocities, extinction limits, and flammability limit, in: Proceedings of the 25th Symposium on Combustion, The Combustion Institute, 1994, pp. 1309–1315.
[8] I. Wierzba, S.O. Bade Shrestha, G.A. Karim, An approach for predicting the flammability limits of fuel/diluent mixtures in air, J. I. Energy 69 (1996) 122–130.
[9] Y.N. Shebeko, W. Fan, I.A. Bolodian, V.Y. Navzenya, An analytical evaluation of flammability limits of gaseous mixtures of combustible-oxidizer-diluent, Fire Safety J. 37 (2002) 549–568.
[10] F. Van den Schoor, F. Verplaetsen, The upper flammability limit of methane/hydrogen/air mixtures at elevated pressures and temperatures, Int. J. Hydrogen Energy 32 (2007) 2548–2552.
[11] CHEM1D, A One-dimensional Laminar Flame Code, Eindhoven University of Technology. Available from: http://www.combustion.tue.nl/chem1d.
[12] Y.A. Çengel, M.A. Boles, Thermodynamics: An Engineering Approach, third ed., WCB/McGraw-Hill, Boston, 1998.
[13] B. Somers, The Simulation of Flat Flames with Detailed and Reduced Chemical Models, Ph.D. Thesis, Eindhoven University of Technology, 1994.
[14] G.P. Smith, D.M. Golden, M. Frenklach, N.W. Moriarty, B. Eiteneer, M. Goldenberg, C.T. Bowman, R. Hanson, S. Song, W.C. Gardiner Jr., V. Lissianski, Z. Qin, GRI 3.0. Available from: http://www.me.berkeley.edu/gri-mech.
[15] A.A. Konnov, Detailed reaction mechanism for small hydrocarbons combustion. Release 0.5. Available from: http://homepages.vub.ac.be/∼akonnov.
[16] J. Appel, H. Bockhorn, M. Frenklach, Kinetic modeling of soot formation with detailed chemistry and physics: laminar premixed flames of C_2 hydrocarbons, Combust. Flame 121 (2000) 122–136, http://www.me.berkeley.edu/soot/mechanisms/mechanisms.html.
[17] K.J. Hughes, T. Turányi, A.R. Clague, M.J. Pilling, Development and testing of a comprehensive chemical mechanism for the oxidation of methane, Int. J. Chem. Kinet. 33 (2001) 513–538, http://www.chem.leeds.ac.uk/Combustion/Combustion.html.
[18] X.J. Gu, Laminar burning velocity and Markstein lengths of methane-air mixtures, Combust. Flame 121 (2000) 41–58.
[19] K.J. Bosschaert, L.P.H. de Goey, The laminar burning velocity of flames propagating in mixtures of hydrocarbons and air measured with the heat flux method, Combust. Flame 136 (2004) 261–269.
[20] J. Buckmaster, D. Mikolaitis, A flammability limit model for upward propagation through lean methane/air mixtures in a standard flammability tube, Combust. Flame 45 (1982) 109–119.
[21] P.D. Ronney, Understanding combustion processes through microgravity research, in: Proceedings of the 27th Symposium on Combustion, The Combustion Institute, 1998, pp. 2485–2506.
[22] S. Crescitelli, G. Russo, V. Tufano, F. Napolitano, L. Tranchino, Flame propagation in closed vessels and flammability limits, Combust. Sci. Technol. 15 (1977) 201–212.
[23] C.K. Law, Propagation, structure, and limit phenomena of laminar flames at elevated pressures, Combust. Sci. Technol. 178 (2006) 335–360.
[24] F. Van den Schoor, F. Verplaetsen, J. Berghmans, Calculation of the upper explosion limit of methane-air mixtures at elevated pressures and temperatures, in: Proceedings of the 12th International Symposium on Loss Prevention and Safety Promotion in the Process Industries, 2007.